Article

Interplay among Tetrahedrane, Butterfly Diradical, and Planar Rhombus Structures in the Chemistry of the Binuclear Iron Carbonyl Phosphinidene Complexes Fe(CO)(PX)

Ioan Silaghi-Dumitrescu, Thomas E. Bitterwolf, and R. Bruce King

J. Am. Chem. Soc., **2008**, 130 (3), 901-906 • DOI: 10.1021/ja0748229

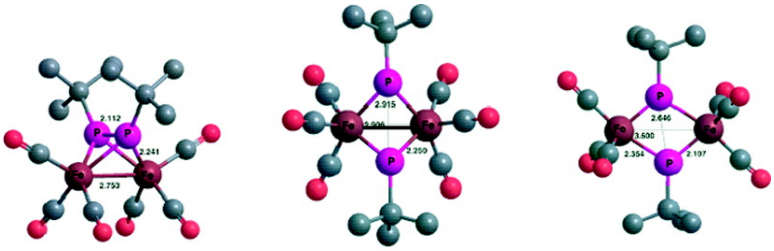

More About This Article

Additional resources and features associated with this article are available within the HTML version:

- Supporting Information
- Access to high resolution figures
- Links to articles and content related to this article
- Copyright permission to reproduce figures and/or text from this article

View the Full Text HTML

J|A|C|S
ARTICLES
Published on Web 12/29/2007

Interplay among Tetrahedrane, Butterfly Diradical, and Planar Rhombus Structures in the Chemistry of the Binuclear Iron Carbonyl Phosphinidene Complexes $Fe_2(CO)_6(PX)_2$

Ioan Silaghi-Dumitrescu,[§] Thomas E. Bitterwolf,[‡] and R. Bruce King*,[||]

Faculty of Chemistry and Chemical Engineering, Babeş-Bolyai University, Cluj-Napoca, Romania, Department of Chemistry, University of Idaho, Moscow, Idaho 83843, and Department of Chemistry and Center for Computational Chemistry, University of Georgia, Athens, Georgia 30602

Received June 30, 2007; E-mail: rbking@chem.uga.edu

Abstract: Density functional theory studies on a series of $Fe_2(CO)_6(PX)_2$ derivatives show the tetrahedrane to be the most stable for the alkyl (X = Me, ^{t}Bu), P−H (X = H), and chloro (X = Cl) derivatives. However, butterfly diradical and planar rhombus structures are found to be more stable than tetrahedranes for the amino (X = NH_2, NMe_2, and N^{i}Pr$_2$) and aryloxy (R = 2,6-^{t}Bu$_2$-4-Me-C_6H_2O) derivatives. For the chloro (X = Cl) and methoxy (X = OMe) derivatives energetically accessible bishomotetrahedrane $Fe_2(CO)_6P_2(\mu\text{-}X)_2$ isomers are observed in which the X substituents on the phosphorus atoms interact with the iron atom to form two direct Fe−X bonds at the expense of two of the four Fe−P bonds. In addition, the global minimum for the hydroxy (X = OH) derivative is an unusual FeP-butterfly structure with a central Fe−P bond as well as two external Fe−P bonds, one external P−P bond, and one external Fe═Fe double bond. Comparison of calculated with experimental ν(CO) frequencies shows that low-temperature Nujol matrix photolysis of (^{i}Pr$_2$NP)$_2$COFe$_2$(CO)$_6$ leads to a planar rhombus rather than a tetrahedrane isomer of $Fe_2(CO)_6(PN^iPr_2)_2$.

1. Introduction

The iron carbonyl sulfide,[1] $Fe_2(CO)_6(\mu\text{-}S_2)$ (**I**) has become a very useful synthon in metal carbonyl chemistry[2] as well as a model for the [FeFe]-only hydrogenase from *C. pasteurianum*.[3] X-ray diffraction indicates $Fe_2(CO)_6(\mu\text{-}S_2)$ to have the tetrahedrane structure (Figure 1, E = S) with Fe−Fe and S−S bond distances of 2.55 Å and 2.01 Å, respectively.[4] We have recently shown by infrared spectroscopy and density functional theory (DFT) computations[5] that photolysis of $Fe_2(CO)_6(\mu\text{-}S_2)$ in a Nujol matrix results in cleavage of its S−S bond to give a butterfly diradical (Figure 1, E = S) analogous to the $(R_2PBR'_2)_2$ singlet diradicals isolated by Bertrand and co-workers[6] as well as closely related $(RPCR')_2$ and $(RNGeR')_2$ species.[7,8] This $Fe_2(CO)_6(\mu\text{-}S_2)$ butterfly diradical appears to be an intermediate in the known [2+2] cycloadditions of the $Fe_2(CO)_6(\mu\text{-}S_2)$ tetrahedrane with a variety of substrates including alkenes,[9] alkynes,[10] and even fullerenes[11] as well as photochemical insertion of CO into the S−S bond.[12]

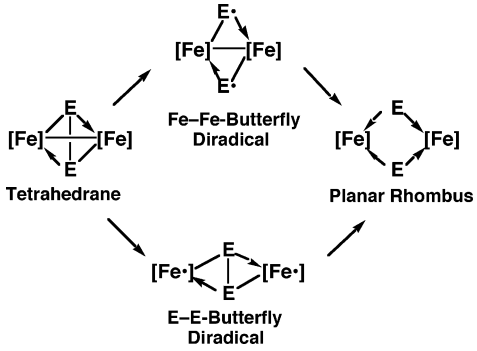

Figure 1. The four fundamental types of structures for $Fe_2(CO)_6E_2$ complexes ([Fe] = $Fe(CO)_3$; E = S, PX; X = Me, ^{t}Bu, NH_2, NMe_2, N^{i}Pr$_2$, OH, OMe, Cl).

The work described in this paper uses similar matrix isolation spectroscopic methods combined with DFT calculations to

[§] Babeş-Bolyai University.
[‡] University of Idaho.
[||] University of Georgia.

(1) Hieber, W.; Gruber, J. Z. *Anorg. Allg. Chem.* **1958**, *296*, 91.
(2) King, R. B.; Bitterwolf, T. E. *Coord. Chem. Rev.* **2000**, *206*−*207*, 563.
(3) Peters, J. W.; Lanzilotta, W. N.; Lemon, B. J.; Seefeldt, L. C. *Science* **1998**, *282*, 1853.
(4) (a) Wei, C. H.; Dahl, L. F. *Inorg. Chem.* **1965**, *4*, 1. (b) Eremenko, K. L.; Berke, H.; van der Zeijden, A. A. H.; Kolobkov, B. I.; Novotorstev, V. M. J. *Organomet. Chem.* **1994**, *471*, 123.
(5) Silaghi-Dumitrescu, I.; Bitterwolf, T. E.; King, R. B. *J. Am. Chem. Soc.* **2006**, *128* (16), 5342.
(6) (a) Scheschkewitz, D.; Amii, H.; Gornitzka, H.; Schoeller, W. W.; Bourissou, D.; Bertrand, G. *Science* **2002**, *295*, 1880. (b) Scheschkewitz, D.; Amii, H.; Gornitzka, H.; Schoeller, W. W.; Bourissou, D.; Bertrand, G. *Angew. Chem., Int. Ed.* **2004**, *43*, 585. (c) Amil, H.; Vranicar, L.; Gornitzka, H.; Bourissou, D.; Bertrand, G. *J. Am. Chem. Soc.* **2004**, *126*, 1344. (d) Cheng, M.-J.; Hu, C.-N. *Mol. Phys.* **2003**, *101*, 1319.
(7) Sebastian, M.; Nieger, M.; Szieberth, D.; Nyulászi, L.; Niecke, E. *Angew Chem. Int. Ed.* **2004**, *43*, 637.
(8) Cui, C.; Brynda, M.; Olmstead, M. M.; Power, P. P. *J. Am. Chem. Soc.* **2004**, *126*, 6510.
(9) Kramer, A.; Lorenz, I. P. *J. Organomet. Chem.* **1990**, *388*, 187 and references cited therein.
(10) Seyferth, D.; Henderson, R. S. *J. Organomet. Chem.* **1991**, *419*, 113.
(11) Westmeyer, M. D.; Galloway, C. P.; Rauchfuss, T. B. *Inorg. Chem.* **1994**, *33*, 4615.
(12) Messelhäuser, J.; Gutenson, K. U.; Lorenz, I.-P.; Hiller, W. J. *Organomet. Chem.* **1987**, *321*, 377.

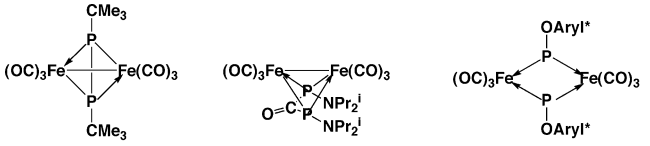

$Fe_2(CO)_6(P^tBu)_2$ (1) (tetrahedrane) | $(^iPr_2NP)_2COFe_2(CO)_6$ (2) (P-bridging CO derivative) | $Fe_2(CO)_6(POAryl^*)_2$ (3) (planar rhombus)

Figure 2. Examples of a tetrahedrane $Fe_2(CO)_6(PR)_2$, a phosphorus-bridging carbonyl derivative $(R_2NP)_2COFe_2(CO)_6$, and a planar rhombus $Fe_2(CO)_6(POR)_2$ (R = 2,6-^{t}Bu$_2$-4-Me$-C_6H_2$) derivative that have been isolated as stable molecules and structurally characterized by X-ray diffraction.

explore closely related $Fe_2(CO)_6(PX)_2$ derivatives in which the sulfur atoms in $Fe_2(CO)_6S_2$ are replaced by isoelectronic phosphinidene units. Such replacement of sulfur by phosphorus generates two external sites where the properties of the Fe_2P_2 cluster can be tuned by modifying the terminal phosphorus substituents. In this connection sample systems with alkyl, dialkylamino, hydroxy, alkoxy, and chloro substituents on the phosphorus atoms have been investigated with the objective of assessing the effects of the terminal groups bonded to phosphorus on the relative stabilities of the tetrahedrane, butterfly diradical, and planar rhombus $Fe_2(CO)_6(PX)_2$ isomers (Figure 1). This study of relatively unstable Fe_2P_2 reaction intermediates provides fundamental understanding of a number of observations in synthetic iron carbonyl chemistry including the following:

(1) The tetrahedrane $Fe_2(CO)_6(P^tBu)_2$ (**1** in Figure 2) can be isolated as a stable molecule, but it reacts at 80 °C with CO, ethylene, and H_2 undergoing rupture of its P−P bond.[13]

(2) Unsaturated organic molecules (e.g., ketones, nitriles, maleic anhydride, norbornadiene, etc.) react thermally with the phosphorus-bridging carbonyl derivative $(^iPr_2NP)_2COFe_2(CO)_6$ (**2** in Figure 2) with extrusion of the phosphorus-bridging CO group and addition of the phosphorus atoms across a C═O, C≡N, or C═C bond in the organic substrate.[14] However, a stable tetrahedrane $Fe_2(CO)_6(N^iPr_2)_2$ (Figure 1, E = PN^iPr_2) has never been isolated, even by heating $(^iPr_2NP)_2COFe_2(CO)_6$ in the absence of a substrate.

(3) A stable compound $Fe_2(CO)_6(POC_6H_2$-4-Me-2,6-^{t}Bu$_2)_2$, with a bulky aryl group (Aryl*) has been shown by X-ray crystallography to have a planar rhombus structure.[15]

2. Experimental and Theoretical Methods

2.1. Photochemistry. A solution of $(^iPr_2NP)_2COFe_2(CO)_6$ in Nujol was applied to CaF_2 windows, which were mounted in a low-temperature cryostat as previously described.[16] After freezing the sample with liquid nitrogen the cell was evacuated to 10^{-2} Torr. Photolysis of the sample was carried out with a 350 W high-pressure mercury lamp using optical filters. Infrared spectra were recorded on a Perkin-Elmer Spectrum 1000 FTIR spectrometer.

2.2. Theoretical Studies. Geometry optimizations on the model compounds were carried out at the B3LYP/6-311G(d)[17−20] and BP86/6-311G(d)[21,22] levels with triple-ζ quality basis functions extended with one set of polarization (d) functions. The Gaussian 98 package has been used with the default fine grid (75302) for evaluating the integrals and the tight (10^{-8}) hartree criterion for the SCF convergence. Whenever large imaginary frequencies (>100i cm^{-1})[23] were calculated, the corresponding normal modes were followed to locate the genuine minima characterized by the absence of imaginary frequencies. The calculations included besides the model species two real systems (X = OAr*, N^iPr_2). In these cases owing to the size of the molecules, we resorted to the ONIOM(B3LYP/6-311G(d):UFF) method,[24,25] selecting the $Fe_2(CO)_6$ core and the P−aryl ring (and P−N fragment) in the high level group. All of the starting geometries for the model systems were built within Spartan 04[26] and preoptimized at the B3LYP/LACVP* level.

DFT optimizations were performed on both the singlet and triplet isomers of the compounds discussed in this paper. In general, the energies of the triplet isomers were found to be higher than those of the corresponding singlet isomers. Therefore, the triplet isomers do not appear to play a significant role in the chemistry discussed in this paper.

For brevity the tetrahedron, Fe−Fe-butterfly, P−P-butterfly, and rhombus isomers (Figure 1) of an $Fe_2(CO)_6(PX)_2$ derivative are designated as *tet*-$Fe_2(CO)_6(PX)_2$, *Fe-but*-$Fe_2(CO)_6(PX)_2$, *P-but*-$Fe_2(CO)_6(PX)_2$, and *rhomb*-$Fe_2(CO)_6(PX)_2$, respectively.

3. Results and Discussion

3.1. $Fe_2(CO)_6(PR)_2$ (R = Me, ^{t}Bu, H). Table 1 summarizes our results on the alkylphosphinidene isomers $Fe_2(CO)_6(PR)_2$ as well as the corresponding P−H derivative $Fe_2(CO)_6(PH)_2$. The methylphosphinidene derivative $Fe_2(CO)_6(PMe)_2$ was chosen as the simplest example of a compound of this type. The *tert*-butylphosphinidene $Fe_2(CO)_6(P^tBu)_2$ derivative was also studied since its tetrahedrane isomer has been synthesized and characterized structurally by Vahrenkamp et al.[13]

Three isomers were found for all three $Fe_2(CO)_6(PR)_2$ derivatives (Figure 3). The tetrahedrane isomers are the global minima in all three cases. They are characterized by a 2.77 ± 0.03 Å Fe−Fe bonding distance and four equal 2.24 Å Fe−P bonding distances. The P−P distances depend on the external phosphorus substituents ranging from 2.112 Å for R = ^{t}Bu to 2.207 Å for R = H. The calculated bond distances in the Fe_2P_2 tetrahedron for *tet*-$Fe_2(CO)_6(P^tBu)_2$ are close to those found by X-ray diffraction by Vahrenkamp et al.[13] (Table 1).

The angles in the Fe_2P_2 rhombus in the *rhomb*-$Fe_2(CO)_6(PR)_2$ isomers deviate considerably from 90° since the nonbonding Fe···Fe and P···P distances across the diagonals of the rhombus are very different, namely 3.60 and 2.60−2.65 Å, respectively. Thus the P−Fe−P angle found in the optimized rhombus structure of $Fe_2(CO)_6(P^tBu)_2$ is 72.5° (Figure 3). Also the rhombuses in these structures are not ideal rhombuses with four equal sides since the four Fe−P distances alternate between 2.10 ± 0.01 and 2.34 ± 0.01 Å. This arises from the fact that two Fe−P bonds involve axial positions and the other two Fe−P bonds involve equatorial positions in the $Fe(CO)_3P_2$ coordination trigonal bipyramid. Thus it is not necessary to invoke a Jahn−Teller distortion similar to that in singlet cyclobutadiene to account for this bond nonequivalence.

3.2. $Fe_2(CO)_6(PNR_2)_2$ (R = H, Me, ^{i}Pr). Table 2 summarizes our results with the aminophosphinidene isomers $Fe_2(CO)_6$-

(13) De, R. L.; Wolters, D.; Vahrenkamp, H. *Z. Naturforsch., B* **1986**, *41*, 283.
(14) Li, Y. W.; Newton, M. G.; King, R. B. *Inorg. Chem.* **1993**, *32*, 5720.
(15) Flynn, K. M.; Bartlett, R. A.; Olmstead, M. M.; Power, P. P. *Organometallics* **1986**, *5*, 813.
(16) Bays, T. J.; Bitterwolf, T. E.; Lott, K. A.; Ollino, M. A.; Rest, A. J.; Smith, L. M. *J. Organomet. Chem.* **1998**, *554*, 75.
(17) Becke, A. D. *J. Chem. Phys.* **1993**, *98*, 5648.
(18) Lee, C.; Yang, W.; Parr, R. G. *Phys. Rev., B* **1988**, *37*, 785.
(19) Vosko, S. H.; Wilk, L.; Nusair, M. *Can. J. Phys.* **1980**, *58*, 1200.
(20) Stephens, P. J.; Devlin, F. J.; Chabalowski, C. F.; Frisch, M. J. *J. Phys. Chem.* **1994**, *98*, 11623.
(21) Becke, A. D. *Phys. Rev., A* **1988**, *38*, 3098.
(22) Perdew, J. P. *Phys. Rev., B* **1986**, *33*, 8822.
(23) Xie, Y.; Schaefer, H. F., III; King, R. B. *J. Am. Chem. Soc.* **2000**, *122*, 8746.
(24) Svensson, M.; Humbel, S.; Froese, R. D. J.; Mastubara, T.; Sieber, S.; Morokuma, K. *J. Phys. Chem.* **1996**, *100*, 19357.
(25) Dapprich, S.; Komaromi, I.; Byun, K. S.; Morokuma, K.; Frisch, M. J. *J. Mol. Struct. (Theochem)* **1999**, 461, 1.
(26) *Spartan'04;* Wavefunction Inc: Irvine, CA, 2004.

Table 1. DFT Studies on the Isomers of $Fe_2(CO)_6(PR)_2$ (R = Me, ^{t}Bu, H)

compound	sym	rel energy	distances (Å)			imaginary frequency cm^{-1}
			Fe–Fe	P–P	Fe–P	
tet-$Fe_2(CO)_6(PMe)_2$	C_{2v}	0.0	2.799	2.148	2.238	none
Fe-but-$Fe_2(CO)_6(PMe)_2$	C_{2v}	10.6	2.823	2.914	2.248	42i
rhomb-$Fe_2(CO)_6(PMe)_2$	C_2	18.9	3.600	2.605	2.103, 2.338	none
tet-$Fe_2(CO)_6(P^tBu)_2$	C_{2v}	0.0	2.753	2.112	2.241	6i
experimental data[13]			2.740	2.059	2.222 (av)	
rhomb-$Fe_2(CO)_6(P^tBu)_2$	C_i	24.3	3.600	2.646	2.107, 2.354	5i
Fe-but-$Fe_2(CO)_6(P^tBu)_2$	C_{2v}	27.1	2.906	2.915	2.250	
tet-$Fe_2(CO)_6(PH)_2$	C_s	0.0	2.771	2.207	2.235	none
Fe-but-$Fe_2(CO)_6(PH)_2$	C_{2v}	4.5	2.862	2.883	2.252	38i
rhomb-$Fe_2(CO)_6(PH)_2$	C_i	22.0	3.614	2.635	2.113, 2.353	9i

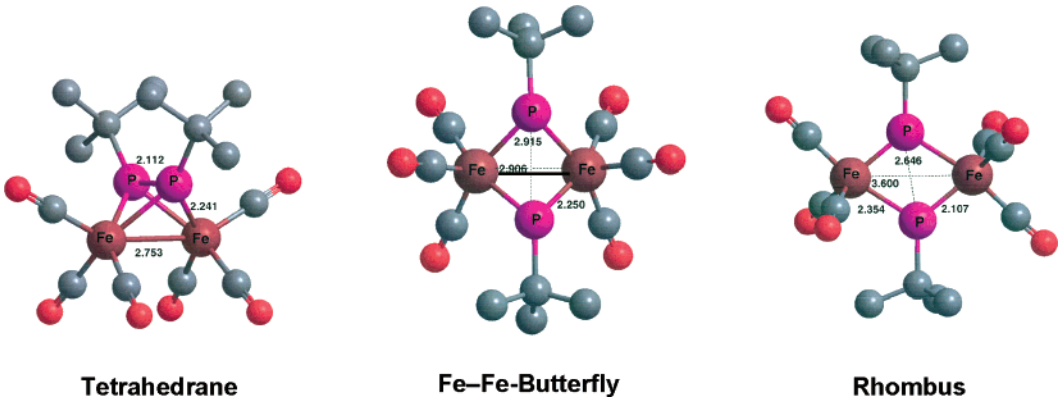

Figure 3. The three isomers of $Fe_2(CO)_6(P^tBu)_2$.

Table 2. The Isomers of $Fe_2(CO)_6(PNR_2)_2$ (R = H, Me, ^{i}Pr)

compound	sym	rel energy	distances (Å)			imaginary frequency cm^{-1}
			Fe–Fe	P–P	Fe–P	
Fe-but-$Fe_2(CO)_6(PNH_2)_2$	C_1	0.0	2.799	2.925	2.099, 2.389	none
rhomb-$Fe_2(CO)_6(PNH_2)_2$	C_1	3.8	3.607	2.502	2.119, 2.269	none
tet-$Fe_2(CO)_6(PNH_2)_2$	C_{2v}	14.1	2.715	2.120	2.236	none
Fe-but-$Fe_2(CO)_6(PNMe_2)_2$	C_1	0.0	2.771	2.892	2.12, 2.38 (av)	none
rhomb-$Fe_2(CO)_6(PNMe_2)_2$	C_1	1.7	3.605	2.573	2.141, 2.286	none
rhomb-$Fe_2(CO)_6(PN^iPr_2)_2$	C_s	0.0	3.570	2.636	2.136, 2.300	
Fe-but-$Fe_2(CO)_6(PN^iPr_2)_2$	C_2	16.9	2.739	2.852	2.10, 2.41 (avg)	

$(PNR_2)_2$. The derivatives $Fe_2(CO)_6(PNH_2)_2$ and $Fe_2(CO)_6(PNMe_2)_2$ were studied as the simplest examples of this type of complex. The diisopropylaminophosphinidene derivative $Fe_2(CO)_6(PN^iPr_2)_2$ was also studied because of its apparent involvement in the phosphorus-bridging carbonyl extrusion chemistry of $(^iPr_2NP)_2COFe_2(CO)_6$ summarized in Figure 4.[27]

The Fe-butterfly and rhombus isomers (Table 2) were found for all three $Fe_2(CO)_6(PNR_2)_2$ derivatives (R = H, Me, ^{i}Pr). The geometries of these $Fe_2(CO)_6(PNR_2)_2$ isomers are very similar to those of the corresponding $Fe_2(CO)_6(PR)_2$ isomers. Thus for the Fe-butterfly $Fe_2(CO)_6(PNR_2)_2$ isomers the Fe−Fe bonding distances, the P···P nonbonding distances, and the Fe−P bonding distances fall in the ranges 2.76 ± 0.04, 2.89 ± 0.04, and 2.11 ± 0.01/2.39 ± 0.02 Å, respectively. For the rhombus $Fe_2(CO)_6(PNR_2)_2$ isomers the alternating Fe−P bonding distances are 2.12 ± 0.02 and 2.28 ± 0.02 Å and the Fe···Fe and P···P nonbonding distances are 3.58 ± 0.02 and 2.57 ± 0.06 Å, respectively. Thus the geometries of these structures appear to be rather insensitive to the substituents on the nitrogen atoms in the $Fe_2(CO)_6(PNR_2)_2$ derivatives in accord with expectation.

The tetrahedrane isomers are found to be significantly destabilized when alkyl groups on phosphorus are replaced by dialkylamino groups. The only $Fe_2(CO)_6(PNR_2)_2$ derivative for which a tetrahedrane isomer was found was $Fe_2(CO)_6(PNH_2)_2$ and even that tetrahedrane isomer was higher in energy than either the corresponding Fe-butterfly or rhombus isomer. Thus for $Fe_2(CO)_6(PNR_2)_2$ (R = H, Me) the global minima are the Fe−Fe-butterfly isomers with the corresponding rhombus isomers lying only slightly higher in energy (+3.8 kcal/mol for R = H and +1.7 kcal/mol for R = Me). For the more sterically hindered $Fe_2(CO)_6(PN^iPr_2)_2$ the rhombus isomer is the global minimum with the corresponding Fe−Fe-butterfly isomer at significantly higher energies (+16.9 kcal/mol). *This explains why a tetrahedrane tet-$Fe_2(CO)_6(PN^iPr_2)_2$ isomer analogous to the Vahrenkamp compound*[13] *tet-$Fe_2(CO)_6(P^tBu)_2$ was never observed in the phosphorus-bridging carbonyl extrusion chemistry of $(^iPr_2NP)_2COFe_2(CO)_6$.*[14]

(27) Li, Y. W.; Newton, M. G.; King, R. B. *Inorg. Chem.* **1993**, *32*, 5720.

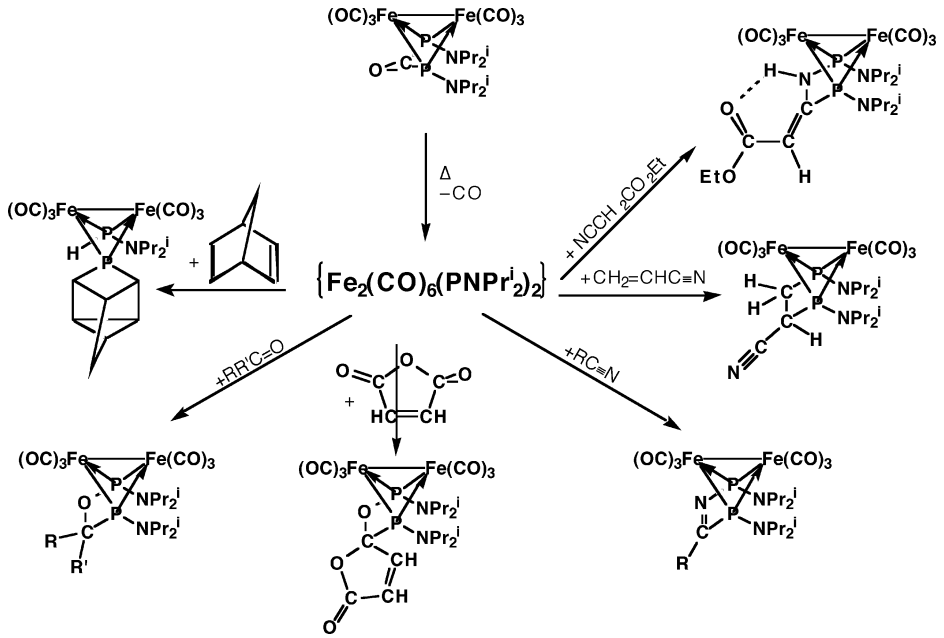

Figure 4. Some reactions of the $Fe_2(CO)_6(PN^iPr_2)_2$ intermediate generated by pyrolysis of $(^iPr_2NP)_2COFe_2(CO)_6$ in the presence of various substrates.

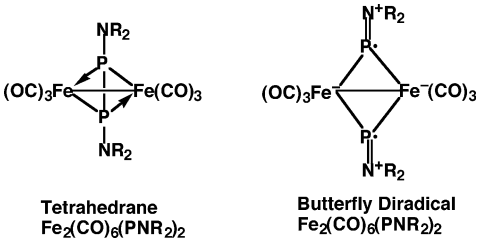

Figure 5. Destabilization of the P−P bond in a tetrahedrane $Fe_2(CO)_6(PNR_2)_2$ by the R_2N substituents.

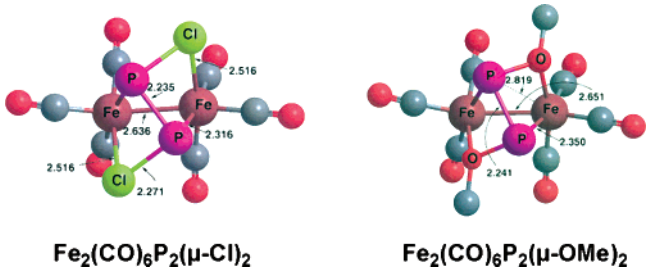

Figure 6. Comparison of the bishomotetrahedrane structures for $Fe_2(CO)_6P_2(\mu\text{-}X)_2$ (X = Cl, OMe).

These DFT results indicate that a P−P bond is destabilized by dialkylamino substituents on the phosphorus. This destabilization can be rationalized by partial P═N double bonding as depicted in Figure 5. Thus the unpaired electrons in the diradical structure are delocalized in the phosphorus−nitrogen double bonds rather than simply localized on the phosphorus atoms.

3.3. $Fe_2(CO)_6(PCl)_2$. The tetrahedrane structure is found to be the lowest energy isomer for $Fe_2(CO)_6(PCl)_2$ as is the case for the alkylphosphinidene derivatives $Fe_2(CO)_6(PR)_2$ (R = Me, ^{t}Bu) discussed above (Table 3). However, this tetrahedrane structure for $Fe_2(CO)_6(PCl)_2$ is distorted so that two of the four Fe−P bonds are 0.14 Å longer than the other two Fe−P bonds. A planar rhombus structure is also found for $Fe_2(CO)_6(PCl)_2$ at 9.4 kcal/mol above *tet*-$Fe_2(CO)_6(PCl)_2$. A third structure found for $Fe_2(CO)_6(PCl)_2$ is an unusual bishomotetrahedrane structure (Figure 6) in which the chlorine atoms are bridges between phosphorus and iron atoms. Thus in this last bishomotetrahedrane structure $Fe_2(CO)_6P_2(\mu\text{-}Cl)_2$, one edge of the tetrahedron is an Fe−Fe bond, one edge is a P−P bond, and two edges are Fe−P bonds. The remaining two edges have a chlorine atom bridging between Fe and P with a nonbonding Fe···P distance of 2.919 Å (Table 3). No butterfly diradical structures for $Fe_2(CO)_6(PCl)_2$ were found.

The $Fe_2(CO)_6(PCl)_2$ system is found to be different from the $Fe_2(CO)_6(PX)_2$ systems discussed above (X = R and NR_2) since a bishomotetrahedrane isomer (Figure 6) is found rather than a butterfly diradical isomer. However, a hypothetical butterfly diradical isomer of $Fe_2(CO)_6(PCl)_2$ can easily convert to the observed bishomotetrahedrane isomer by breaking one of the two Fe−P bonds on each iron and replacing them with Fe−Cl bonds (Figure 7). This process converts the unpaired electrons on the phosphorus atoms in the butterfly diradical structure into electron pairs. The formation of an energetically accessible bishomotetrahedrane isomer of $Fe_2(CO)_6(PCl)_2$ shows how the external groups bonded to phosphorus can influence the isomer distribution in $Fe_2(CO)_6(PX)_2$ systems by forming Fe−X bonds.

Table 3. The Isomers of $Fe_2(CO)_6(PCl)_2$

			distances (Å)			
compound	sym	rel energy	Fe–Fe	P–P	Fe–P	imaginary frequency cm^{-1}
tet-$Fe_2(CO)_6(PCl)_2$	C_1	0.0	2.821	2.250	2.150 (P), 2.290 (P)	none
rhomb-$Fe_2(CO)_6(PCl)_2$	C_s, C_i	9.4	3.652	2.501	2.079 (P), 2.340 (P)	12i
$Fe_2(CO)_6P_2(\mu\text{-}Cl)_2$	C_2	14.4	2.636	2.235	2.316 (P), 2.516 (Cl)	none

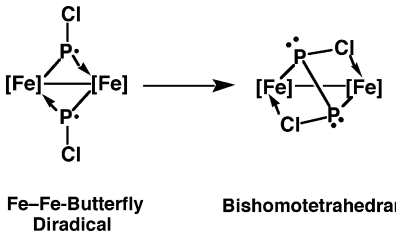

Figure 7. Conversion of the butterfly diradical isomer of $Fe_2(CO)_6(PCl)_2$ to the corresponding bishomotetrahedrane isomer ([Fe] = $Fe(CO)_3$).

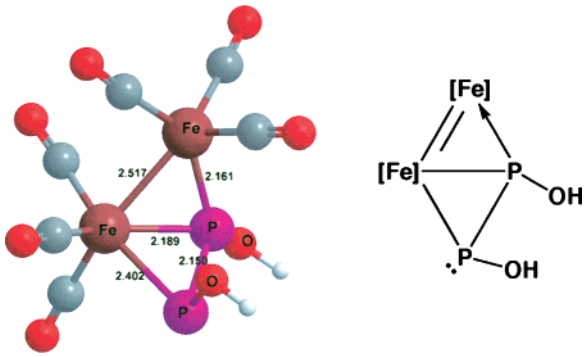

Figure 8. Structure of *FeP-but*-$Fe_2(CO)_6(POH)_2$ ([Fe] = $Fe(CO)_3$).

3.4. $Fe_2(CO)_6(POR)_2$ (R = H, Me, 2,6-^{t}Bu$_2$-4-MeC$_6$H$_2$). The lowest energy isomer found for $Fe_2(CO)_6(POMe)_2$ has a distorted tetrahedrane structure with two "short" Fe−P bonds of 2.07 ± 0.01 Å and two "long" Fe−P bonds of 2.35 ± 0.03 Å as well as a long P−P distance of 2.441 Å for a tetrahedrane structure (Table 4). Close in energy to this global minimum for $Fe_2(CO)_6(POMe)_2$ at +2.0 kcal/mol is an unusual $Fe_2(CO)_6P_2$-(μ-OMe)$_2$ structure (Figure 6) related to the bishomotetrahedrane structure $Fe_2(CO)_6P_2(\mu$-Cl)$_2$ discussed above. In this bishomotetrahedrane structure for $Fe_2(CO)_6P_2(\mu$-OMe)$_2$ two of the four Fe−P distances remain bonding distances at 2.350 Å but the other two Fe···P distances lengthen to 2.819 Å and are bridged by a methoxy oxygen. A rhombus isomer is also found for $Fe_2(CO)_6(POMe)_2$ at 10.1 kcal/mol above the global minimum tetrahedrane.

The global minimum for $Fe_2(CO)_6(POH)_2$ is an unusual unsymmetrical FeP-butterfly structure with a Fe−P bond (2.189 Å) for the "body" of the butterfly (Figure 8a). The external edges of the butterfly consist of an Fe═Fe bond of 2.517 Å, a P−P bond of 2.150 Å, and two Fe−P bonds of 2.161 Å and 2.402 Å. Thus the formation of this unusual FeP-butterfly structure involves breaking a Fe−P bond in the corresponding tetrahedrane rather than a P−P bond. A reasonable nonradical valence bond structure can be drawn for *FeP-but*-$Fe_2(CO)_6(POH)_2$ (Figure 8b) if the iron−iron bond is assumed to be a double bond. This is a reasonable assumption since the Fe═Fe distance of this FeP-butterfly of 2.517 Å is significantly less than the Fe−Fe single bond distances of 2.73−2.80 Å in the Fe-butterflies (Tables 1 and 2).

The only other isomer found for $Fe_2(CO)_6(POH)_2$ is the rhombus isomer. The Fe−P, Fe···Fe, and P···P distances in this rhombus isomer are very similar to those in the closely related rhombus isomer of $Fe_2(CO)_6(OMe)_2$.

3.5. Infrared ν(CO) Frequencies. The $Fe_2(CO)_6(PX)_2$ derivatives exhibit characteristic infrared ν(CO) frequencies around 2000 cm^{-1} so that information of this type is useful in identifying species observed in low-temperature matrix isolation studies. Table 5 summarizes the computed ν(CO) frequencies for the compounds discussed in this paper organized by structure type. Frequencies calculated by the BP86 functional are listed directly, whereas those calculated by the B3LYP functional are scaled by 0.9663.[28] Using the BP86/6-31G(d) method the calculated ν(CO) frequencies for the known *tet*-$Fe_2(CO)_6$-($P^tBu)_2$ are within ±6 cm^{-1} of the experimentally found frequencies (Table 5).[13] Similarly this method gives calculated metal ν(CO) frequencies within ±11 cm^{-1} of the experimental frequencies for (^{i}Pr$_2$NP)$_2$COFe$_2$(CO)$_6$. However, the calculated ν(CO) frequency for the phosphorus-bridging carbonyl group is 51 cm^{-1} higher than the experimental value.

3.6. Generation of $Fe_2(CO)_6(P^iNPr_2)_2$ in a Low-Temperature Matrix. To obtain some insight into the mechanisms of the thermal reactions of the phosphorus-bridging carbonyl (^{i}Pr$_2$NP)$_2$COFe$_2$(CO)$_6$ (**2** in Figure 2) with unsaturated organic molecules (Figure 4), a matrix isolation study was performed using low-temperature photolysis of **2** in a Nujol medium. The results have been presented in a preliminary report.[29] We now present a comparison of our experimentally observed ν(CO) frequencies of this photoproduct with the computed frequencies for suitable model compounds.

The infrared ν(CO) frequencies of (^{i}Pr$_2$NP)$_2$COFe$_2$(CO)$_6$ (**2** in Figure 2) in Nujol at 90 K are found at 2058 (m), 2014 (s), 1992 (m), 1970 (m), 1958 (w), and 1718 (w) cm^{-1} (Figure 9, lower spectrum). The five observed metal carbonyl ν(CO) frequencies are in good agreement with the calculated values using the BP86/6-31G(d) method as discussed above, assuming that the calculated frequencies at 1980 and 1976 cm^{-1} are not resolved in the actual spectrum (Table 5). The lowest energy band at 1718 cm^{-1} in this spectrum corresponds to the phosphorus-bridging CO group. Photolysis of **2** at λ_{irr} > 330 nm was found to have no detectable effect on the spectrum of the compound. However, continuous photolysis in the range

Table 4. The Isomers of $Fe_2(CO)_6(POR)_2$ (R = H, Me, Ar*)

			distances (Å)			
compound	sym	rel energy	Fe–Fe	P–P	Fe–P	imaginary frequency cm^{-1}
FeP-but-$Fe_2(CO)_6(POH)_2$	C_1	0.0	2.517	2.150	2.161, 2.189, 2.402	none
Rhomb-$Fe_2(CO)_6(POH)_2$	C_1	1.5	3.602	2.481	2.084, 2.285	none
tet-$Fe_2(CO)_6(POMe)_2$	C_1	0.0	2.826	2.441	2.07, 2.35 (av)	none
$Fe_2(CO)_6P_2(\mu$-OMe)$_2$	C_2	2.0	2.651	2.241	2.350, 2.819	none
rhomb-$Fe_2(CO)_6(POMe)_2$	C_1	10.1	3.618	2.480	2.090, 2.296	none
rhomb-$Fe_2(CO)_6(POAr^*)_2$	C_i	0.0	3.638	2.461	2.086, 2.300	not calculated
experimental[15]			3.610	2.369	2.113, 2.203	
but-$Fe_2(CO)_6(POAr^*)_2$	C_2	13.3	2.691	2.827	2.193, 2.307	not calculated

Table 5. Metal Carbonyl ν(CO) Frequencies Predicted for the $Fe_2(CO)_6(PX)_2$ Isomers (Infrared Intensities in Parentheses Are in km/mol)

compound	ν(CO) frequencies (cm^{-1})
tet-$Fe_2(CO)_6(P^tBu)_2$ (B3LYP)	2090(920), 2015(2130), 2014(1290), 1993(620), 1990(0), 1983(210)
tet-$Fe_2(CO)_6(P^tBu)_2$ (BP86)	2047(733), 2009 (1364), 1992 (1083), 1971 (541), 1969(0), 1962(331)
tet-$Fe_2(CO)_6(P^tBu)_2$ (exptl)	2053 (m), 2015 (s), 1988 (vs), 1968 (s), 1958 (m)
tet-$Fe_2(CO)_6(PNH_2)_2$ (B3LYP)	2077(679), 2025(1340), 2024 (2260), 2005(703), 2000(0), 1993(239)
Fe-but-$Fe_2(CO)_6(PNH_2)_2$ (B3LYP)	2060(206), 2028(2280), 2012(1270), 2001(1460), 1998(27), 1987(16)
Fe-but-$Fe_2(CO)_6(PNMe_2)_2$ (B3LYP)	2052(420), 2019(2120), 2005(790), 1994(1480), 1990(80), 1973(244)
Fe-but-$Fe_2(CO)_6(PN^iPr_2)_2$ (BP86)	2035(364), 2004(1626), 1980(666), 1976(1088), 1965(3), 1965(129)
rhomb-$Fe_2(CO)_6(PNH_2)_2$ (B3LYP)	2044(4), 2017(2590), 1992(1420), 1989(1200), 1982(727), 1978(293)
rhomb-$Fe_2(CO)_6(PNMe_2)_2$ (B3LYP)	2030(1), 2008(2670), 1978(12), 1978(1260), 1970(2160), 1964(1)
rhomb-$Fe_2(CO)_6(PN^iPr_2)_2$ (BP86)	2017(0), 2000(1851), 1964(867), 1963(0), 1957(1596), 1952(0)
rhomb-$Fe_2(CO)_6(POMe)_2$ (B3LYP)	2060(0), 2039(2440), 2008(0), 2004(1570), 1987(2040), 1981(0)
rhomb-$Fe_2(CO)_6(POAr^*)_2$ (exptl)	2052 (sh), 2041 (sh), 2021 (s), 2007 (s), 1991 (s), 1961 (s)
$(^iPr_2NP)_2COFe_2(CO)_6$ (BP86)	2052(540), 2018(1229), 1997(993), 1980(220), 1976(352), 1969(284), 1769(344)
$(^iPr_2NP)_2COFe_2(CO)_6$ (exptl)	2058 (m), 2014 (s), 1992 (m), 1970 (m), 1958 (m), 1718 (w)

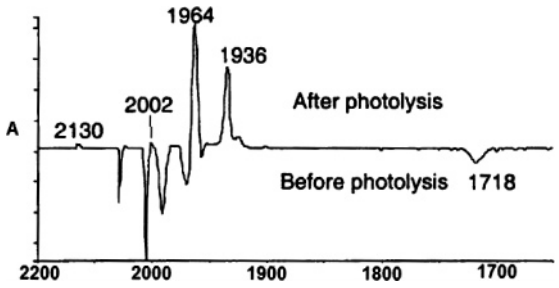

Figure 9. Changes in the infrared spectrum of $(^iPr_2NP)_2COFe_2(CO)_6$ upon photolysis at 220 nm < λ_{irr} < 420 nm.

220−420 nm resulted in bleaching the the bands of **2** with the concurrent appearance of new bands at 2130, 2002 (w), 1964 (s), and 1936 (m) cm^{-1} (Figure 9, upper spectrum). The new band at 2130 cm^{-1} is characteristic of a "free" CO molecule in frozen Nujol. The disappearance of bands in the phosphorus-bridging carbonyl region of **2** suggests that the CO that is lost upon photolysis arises from extrusion of the phosphorus-bridging CO in **2**. Back photolysis at long wavelengths (λ_{irr} > 400 nm) and annealing of the photolyzed samples resulted in complex new spectra that could not be meaningfully interpreted.

The ν(CO) spectrum of the $(^iPr_2NP)_2COFe_2(CO)_6$ (**2**) photoproduct (Figure 9) is characterized by two strong bands and one weaker band. Comparison of this pattern with those calculated for the various $Fe_2(CO)_6(PNR_2)_2$ (R = H, Me) isomers using the BP86/6-31G(d) method (Table 5) supports the formulation of this product as the *rhomb*-$Fe_2(CO)_6(PN^iPr_2)_2$ isomer rather than the corresponding tetrahedrane or butterfly isomers. Thus, the calculated strong ν(CO) frequencies at 2000, 1964, and 1957 cm^{-1} in the infrared ν(CO) spectrum of *rhomb*-$Fe_2(CO)_6(PN^iPr_2)_2$ match very well the experimental frequencies at 2002, 1964, and 1936 cm^{-1} from this matrix isolation experiment. This is consistent with our calculations indicating the rhombus to be the lowest energy of the $Fe_2(CO)_6(PN^iPr_2)_2$ isomers.

(28) Vibrational Frequency Scaling Factors. http://srdata.nist.gov/cccbdb/vsf.asp.
(29) King, R. B.; Bitterwolf, T. E.; Scallorn, W. B.; Weiss, C. A. *Phosphorus, Sulfur, Silicon* **2002**, *177*, 1567.

4. Summary

Density functional theory studies on a series of $Fe_2(CO)_6(PX)_2$ derivatives show the tetrahedrane to be the most stable for the alkyl (X = Me, ^{t}Bu), P−H (X = H), and chloro (X = Cl) derivatives. However, butterfly diradical and planar rhombus structures are found to be more stable than tetrahedranes for the amino (X = NH_2, NMe_2, and N^iPr_2) and aryloxy (R = 2,6-^{t}Bu$_2$-4-Me−C_6H_2) derivatives. For the chloro (X = Cl) and methoxy (X = OMe) derivatives energetically accessible bishomotetrahedrane $Fe_2(CO)_6P_2(\mu\text{-}X)_2$ isomers are observed in which the X substituents on the phosphorus atoms interact with the iron atom to form two direct Fe−X bonds at the expense of two of the four Fe−P bonds. In addition, the global minimum for the hydroxy (X = OH) derivative is an unusual FeP-butterfly structure with a central Fe−P bond as well as two external Fe−P bonds, one external P−P bond, and one external Fe═Fe double bond.

These results are used to interpret data from low-temperature Nujol matrix photolysis experiments on $(^iPr_2NP)_2COFe_2(CO)_6$ (**2**), designed to provide insight into the mechanism of thermal reactions of **2** with organic substrates involving extrusion of the phosphorus-bridging CO group.[14] The resulting $Fe_2(CO)_6(PN^iPr_2)_2$ photoproduct is shown to be the rhombus rather than the tetrahedrane or butterfly isomer by comparison of the calculated ν(CO) frequencies on suitable model compounds with those observed experimentally. Furthermore, these computations account for the failure to observe a tetrahedrane isomer of $Fe_2(CO)_6(PN^iPr_2)_2$ analogous to the stable and well-characterized[13] tetrahedrane isomer of $Fe_2(CO)_6(P^tBu)_2$ (Figure 2).

Acknowledgment. We are indebted to the National Science Foundation for support of this work under Grants CHE-0209857 and CHE-0315226. Part of this work was undertaken with the financial support from CEEX-60/RIOSIN Romania.

JA0748229